Atherosclerosis 238 (2015) 22–25

Contents lists available at ScienceDirect

Atherosclerosis

journal homepage: www.elsevier.com/locate/atherosclerosis

Is it safe to implant bioresorbable scaffolds in ostial side-branch lesions? Impact of 'neo-carina' formation on main-branch flow pattern. Longitudinal clinical observations

Antonios Karanasos [a, 1], Yingguang Li [b, 1], Shengxian Tu [c, b, *], Jolanda J. Wentzel [d], Johan H.C. Reiber [b], Robert-Jan van Geuns [a], Evelyn Regar [a]

[a] Department of Interventional Cardiology, Thoraxcenter, Erasmus University Medical Center, Rotterdam, Netherlands
[b] Division of Image Processing, Department of Radiology, Leiden University Medical Center, Leiden, Netherlands
[c] Biomedical Instrument Institute, School of Biomedical Engineering, Shanghai Jiao Tong University, Shanghai, PR China
[d] Department of Biomedical Engineering, Thoraxcenter, Erasmus University Medical Center, Rotterdam, Netherlands

ARTICLE INFO

Article history:
Received 22 September 2014
Received in revised form
25 October 2014
Accepted 9 November 2014
Available online 18 November 2014

Keywords:
Optical coherence tomography
Bioresorbable vascular scaffold
Primary percutaneous coronary intervention
Computational fluid dynamics
Bifurcation intervention
Atherosclerosis progression

ABSTRACT

Formation of a 'neo-carina' has been reported after bioresorbable vascular scaffolds (BVS) implantation over side-branches. However, as this 'neo-carina' could protrude into the main-branch, its hemodynamic impact remains unknown. We present two cases of BVS implantation for ostial side-branch lesions, and investigate the flow patterns at follow-up and their potential impact. Computational fluid dynamics analysis was performed, using a 3D mesh created by fusion of 3-dimensional angiogram with optical coherence tomography images. In our first case, mild disturbances were seen when 'neo-carina' did not protrude perpendicularly into the main branch. In the second case, extensive flow re-distribution was observed due to a more pronounced protrusion of the 'neo-carina'. Importantly, these areas of hemodynamic disturbance were observed together with lumen narrowing in a non-stenotic vessel segment. Our case observations highlight the importance of investigating the hemodynamic consequences of BVS implantation in bifurcation lesions and illustrate a novel method to do so *in vivo*.

Bioresorbable vascular scaffolds (BVS) are a new treatment for coronary artery disease associated with a favorable long-term healing response with complete strut resorption and restoration of the vascular phenotype [1]. Despite a common misconception that BVS implantation over side-branches is associated with eventual disappearance of jailing struts, morphological changes of side-branch ostia have been reported, with tissue bridge formation resembling a 'neo-carina' [1–3]. 'Neo-carina' formation could be an appealing alternative to metal stents for bifurcation or ostial lesions [4], where non-apposed side-branch struts have been associated with incomplete healing and thrombosis [5,6]. However in ostial lesions, this 'neo-carina' may protrude into the main-branch, potentially influencing the local hemodynamic environment, and especially the main branch flow pattern. We present two cases of BVS implantation for ostial side-branch lesions, and investigate the patterns of flow distribution at follow-up and their potential implications.

For all patients and follow-ups, a 3-dimensional angiogram was created from two angiographic projections using QAngioXA 3D RE (Medis Specials bv, Leiden, Netherlands). In the first patient, selected planes for the 3D angiogram were (1 LAO, 32 Cranial) and (32 LAO, 29 Cranial), and in the second patient (35 RAO, 37 Cranial) and (54 LAO, 26 Cranial). Angle measurement was performed in both cases in the reconstructed 3D angiograms. Computational fluid dynamics (CFD) analysis was subsequently performed, using a 3D mesh created by fusion of the 3-dimensional angiogram with the OCT images [7]. For the CFD simulations, blood was modeled as incompressible Newtonian fluid. The volumetric flow, derived from TIMI frame count and 3D quantitative coronary angiography, was used as the boundary condition at the inlet, while outflow (fully-developed flow) condition was applied at the outlets [8]. Both

* Corresponding author. Room123, Med-X Research Institute, 3 Teaching Building, Shanghai Jiao Tong University, No. 1954, Hua Shan Road, Shanghai 200030, PR China.
E-mail address: sxtu@sjtu.edu.cn (S. Tu).
[1] These authors contributed equally to this work.

http://dx.doi.org/10.1016/j.atherosclerosis.2014.11.013
0021-9150/

subjects have provided informed consent, and the study complies with the declaration of Helsinki.

1. Narrow bifurcation angle

A 73-year old gentleman presenting with acute myocardial infarction received a 2.5 mm × 18 mm BVS at the ostium of a diagonal branch (Fig. 1). OCT showed mild protrusion of the proximal scaffold into the LAD, in the presence of a narrow LAD-diagonal bifurcation angle (31°). CFD analysis performed without taking the protruding struts into consideration showed an evenly distributed flow profile in the mid LAD, with the average flow velocity in the mid LAD being slightly higher than in the diagonal branch. Follow-up OCT was performed 9 months later in the context of a research protocol, while the patient was asymptomatic. OCT showed a good overall healing response and tissue coverage of the protruding struts, leading to formation of a 'neo-carina'. CFD analysis was performed using the 9-month 3D-angiography and OCT fusion model, demonstrating a slightly changed mid LAD flow profile compared to baseline, indicating a modest influence of the 'neo-carina'. Changes included mild flow acceleration near the center of the lumen and mild deceleration at the region of the vessel wall located at the back-side of the 'neo-carina', co-localizing with areas of low wall shear stress.

2. Wide bifurcation angle

A 52 year-old gentleman with acute myocardial infarction received a 2.5 mm × 18 mm BVS at the ostium of the second diagonal branch (Fig. 2). The bifurcation angle (60°) was wider than in the previous case. OCT imaging post-implantation showed, also in this case, an extensive and perpendicular protrusion of the proximal scaffold segment into the LAD. CFD performed in the 3D mesh created by fusion of 3D-angiography and OCT without taking protruding struts into consideration demonstrated even distribution of flow velocities in the two branches. Follow-up OCT was performed 1 year later for a research protocol, while the patient remained asymptomatic. OCT demonstrated extensive tissue coverage of these protruding struts, creating the morphological appearance of a 'neo-carina'. CFD analysis performed using the 12-month fusion model showed a significantly altered flow profile of the mid LAD. Specifically, high flow acceleration was observed opposite to the side-branch ostium [in a relatively narrowed lumen (lumen area: 6.54 mm^2) due to the protrusion of the 'neo-carina' into the main vessel], whereas regions of slow flow velocities and re-circulation were observed at the back-side of the 'neo-carina' and associated with an extensive region of low shear stress at the corresponding wall segments. Importantly, this altered hemodynamic profile was observed in conjunction with lesion progression, consisting of lumen narrowing at the LAD segment distally to the bifurcation.

Contrary to the common misconception that BVS are ideal for bifurcations as they "eventually disappear", 'neo-carina' formation has been described in follow-up of BVS overlying side-branches, as a consequence of tissue coverage and gradual polymer bioresorption [1,2]. At initial stages this 'neo-carina' is comprised by struts covered by tissue in front of the side-branch ostium, whereas at later stages, after complete strut resorption, the 'neo-carina' consists of thin tissue bridges, with signal-rich appearance by OCT [1]. Formation of such 'neo-carinas' has been regarded as potentially favorable, compared to the permanent side-branch jailing from metal stents, considering that the latter has been associated with delayed healing and risk for thrombosis [6]. Nevertheless, the physiological significance of these 'neo-carinas' has not been investigated so far.

Our cases demonstrate for the first time, that 'neo-carina' development after ostial BVS implantation could have adverse hemodynamic consequences by acting as flow dividers that alter the hemodynamics of the main vessel downstream to the bifurcation. Such changes can range widely depending on the extent of protrusion in the main-branch, which is subject to several factors, including bifurcation angle, side-branch diameter, and length of scaffold protrusion. In our cases, both the side-branch diameter and the length of scaffold protrusion were similar (distal reference diameter by 3D-QCA: 3.04 mm and 3.06 mm, respectively; length of protrusion by 2D-OCT: 2.4 mm in both cases), with the bifurcation angle being the main factor differing significantly between cases. In our first case, mild disturbances were seen when 'neo-carina' did not protrude perpendicularly into the main branch, due to a narrow bifurcation angle. In the second case, extensive flow redistribution regions were observed because of the more perpendicular protrusion of the 'neo-carina' as a consequence of a wider bifurcation angle. Of note, these areas of hemodynamic disturbance were observed together with lumen narrowing in a non-stenotic vessel segment, providing pilot observations of a potential impact of device-induced hemodynamic changes on atherosclerosis progression. This observation is in accordance with prospective studies

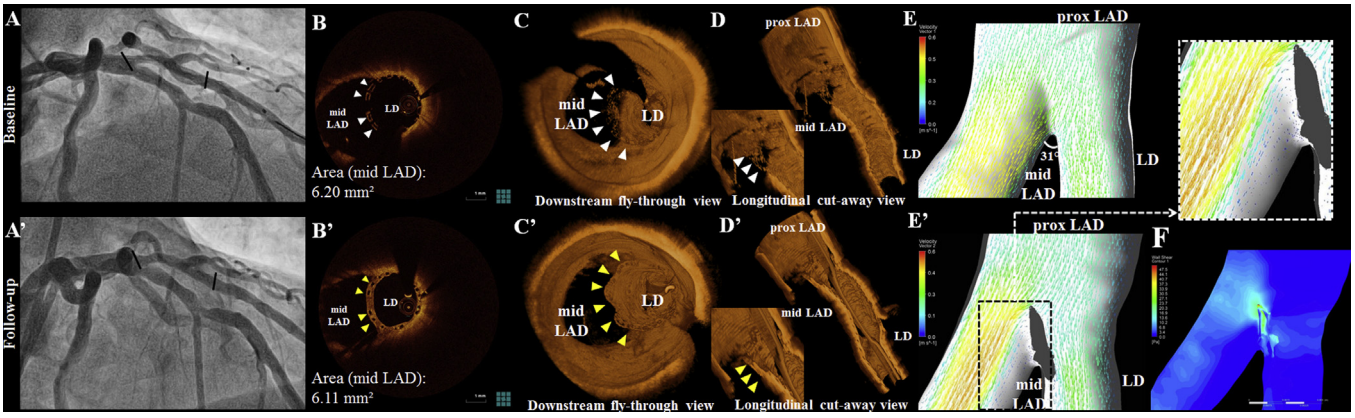

Fig. 1. A–E. (A) Angiogram, (B) 2D-OCT, (C–D) 3D-OCT images, and (E) computational fluid dynamics (CFD) analysis post-implantation. After ostial scaffold implantation at the diagonal branch (LD), scaffold protrusion into the main vessel is observed in cross-sectional and 3D images (white arrowheads), while CFD demonstrates symmetrical flow distribution in the mid left anterior descending artery (LAD). A′–E′. (A′) Angiogram, (B′) 2D-OCT, (C′–D′) 3D-OCT images, and (E′) CFD analysis at 9-month follow-up. (yellow arrowheads). CFD shows a mild increase of flow velocity in mid LAD opposite to the 'neo-carina', with regions of flow deceleration at the backside of the 'neo-carina' (gray area). F. Shear stress profile at 9-month follow-up. (For interpretation of the references to color in this figure legend, the reader is referred to the web version of this article.)

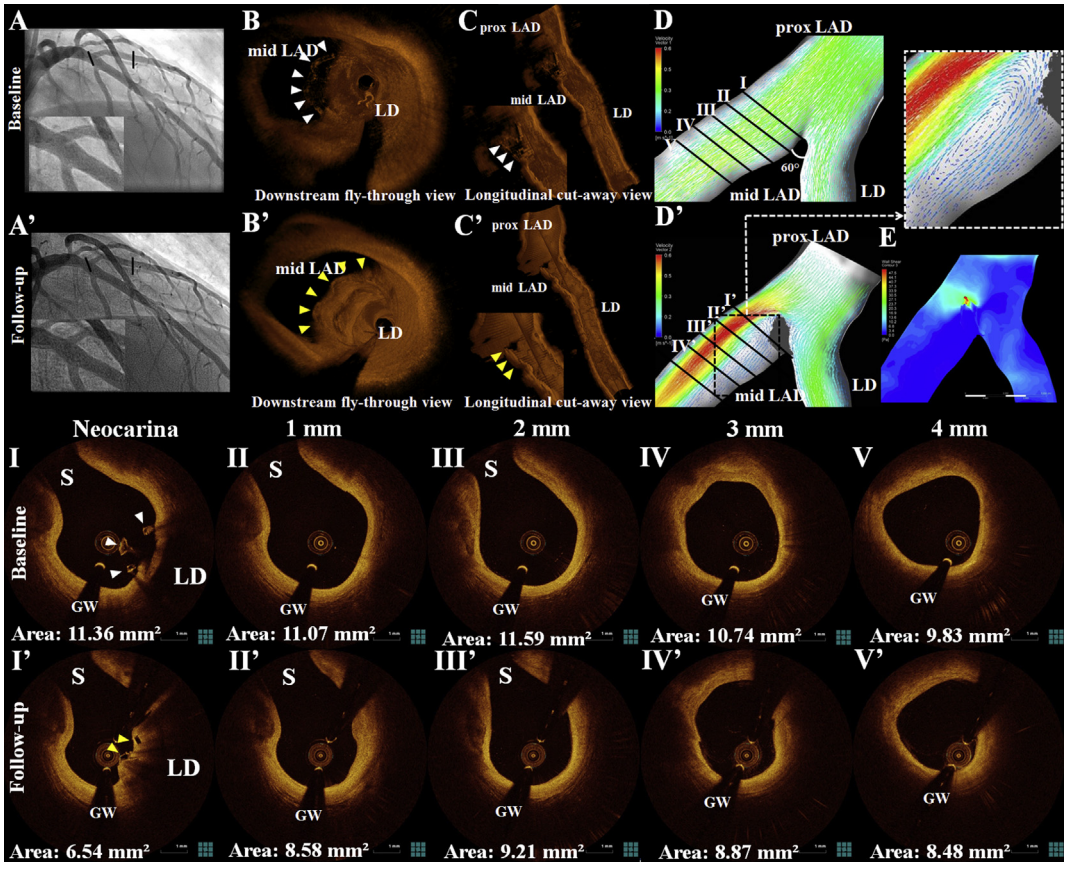

Fig. 2. A–D. (A) Angiogram, (B–C) 3D-OCT images, and (D) computational fluid dynamics (CFD) analysis post-implantation. After ostial scaffold implantation at the diagonal branch (LD), perpendicular scaffold protrusion into the main vessel is observed in the 3D images (white arrowheads), while the CFD analysis demonstrates the symmetrical distribution of flow downstream of the bifurcation. A′–D′. (A′) Angiogram, (B′–C′) 3D-OCT images, and (D′) CFD analysis at 12-month follow-up. Tissue growth over protruding struts has resulted in 'neo-carina' formation (yellow arrowheads). CFD shows substantial flow acceleration opposite to the side-branch ostium in mid LAD, due to the perpendicular 'neo-carina' protrusion (gray area). Conversely, at the backside of the 'neo-carina' there are extensive areas of slow flow and re-circulation. F. Shear stress profile at 12-month follow-up I–V′. Matched 2-dimensional OCT images from a mid-LAD segment downstream to the bifurcation (see D–D′) (I–V) post-implantation and (I′–V′) at 12-month follow-up showing luminal narrowing over time. S = septal, LD = diagonal, GW = guidewire, white arrowheads = protruding struts at baseline, yellow arrowheads = protruding struts at follow-up. (For interpretation of the references to color in this figure legend, the reader is referred to the web version of this article.)

showing the important role of hemodynamic parameters such as low and oscillatory shear stress in lesion progression [9–11].

3. Limitations

Although, our cases suggest the possible contribution of bifurcation angle in determining the extent of 'neo-carina' protrusion into the main branch, larger studies are needed for identifying the exact predictors of excessive protrusion. As our study aimed to investigate the hemodynamic consequences after 'neo-carina' formation, CFD at baseline was performed without considering the protruding struts, in an attempt to demonstrate differences between 'optimal' flow conditions in the absence of any protrusion and actual flow conditions in the presence of the 'neo-carina'. A meticulous modeling incorporating the impact of protruding struts on flow could provide further insight into the mechanisms of 'neo-carina' formation, as hemodynamic factors have been associated with BVS coverage [12]. In any case, the observed follow-up flow patterns are not affected by this amendment in the baseline analysis.

Overall, our case observations highlight the clinical importance of investigating the hemodynamic consequences of BVS implantation in bifurcation lesions and illustrate a novel method to do so *in vivo*. Insights gained from such studies could have a significant impact on treatment strategy selection in bifurcation lesions.

Funding sources

Antonios Karanasos would like to acknowledge the funding support of the Hellenic Heart Foundation and St Jude Medical. Shengxian Tu would like to acknowledge the funding support of the Natural Science Foundation of China under Grant 61271155.

Disclosures

Y Li is employed by Medis Specials bv and has a research appointment at the Leiden University Medical Center (LUMC). S Tu was employed by Medis Specials bv until June 2014. JHC Reiber is the CEO of Medis Specials bv, and has a part-time appointment at Leiden University Medical Center as Professor of Medical Imaging.

References

[1] A. Karanasos, C. Simsek, M. Gnanadesigan, N.S. van Ditzhuijzen, R. Freire, J. Dijkstra, S. Tu, N.M. Van Mieghem, G. van Soest, P. De Jaegere, P.W. Serruys, F. Zijlstra, R.J. Van Geuns, E. Regar, Optical coherence tomography assessment of the long-term vascular healing response 5 years after first-in-man implantation of the everolimus-eluting bioresorbable vascular scaffold, J. Am. Coll. Cardiol. 64 (2014) 2343–2356.

[2] T. Okamura, Y. Onuma, H.M. Garcia-Garcia, E. Regar, J.J. Wykrzykowska, J. Koolen, L. Thuesen, S. Windecker, R. Whitbourn, D.R. McClean, J.A. Ormiston, P.W. Serruys, 3-dimensional optical coherence tomography assessment of

jailed side branches by bioresorbable vascular scaffolds: a proposal for classification, JACC Cardiovasc. Interventions 3 (2010) 836–844.
[3] T. Okamura, P.W. Serruys, E. Regar, Cardiovascular flashlight. The fate of bioresorbable struts located at a side branch ostium: serial three-dimensional optical coherence tomography assessment, Eur. Heart J. 31 (2010) 2179.
[4] V. Dzavik, A. Colombo, The absorb bioresorbable vascular scaffold in coronary bifurcations: insights from bench testing, JACC Cardiovasc. Interventions 7 (2014) 81–88.
[5] A. Farb, A.P. Burke, F.D. Kolodgie, R. Virmani, Pathological mechanisms of fatal late coronary stent thrombosis in humans, Circulation 108 (2003) 1701–1706.
[6] J.L. Gutierrez-Chico, E. Regar, E. Nuesch, T. Okamura, J. Wykrzykowska, C. di Mario, S. Windecker, G.A. van Es, P. Gobbens, P. Juni, P.W. Serruys, Delayed coverage in malapposed and side-branch struts with respect to well-apposed struts in drug-eluting stents: in vivo assessment with optical coherence tomography, Circulation 124 (2011) 612–623.
[7] S. Tu, S.A. Pyxaras, Y. Li, E. Barbato, J.H. Reiber, W. Wijns, In vivo flow simulation at coronary bifurcation reconstructed by fusion of 3-dimensional X-ray angiography and optical coherence tomography, Circ. Cardiovasc. Interventions 6 (2013) e15–17.
[8] S. Tu, E. Barbato, Z. Koszegi, J. Yang, Z. Sun, N.R. Holm, B. Tar, Y. Li, D. Rusinaru, W. Wijns, J.H. Reiber, Fractional flow reserve calculation from 3-dimensional quantitative coronary angiography and TIMI frame count: a fast computer model to quantify the functional significance of moderately obstructed coronary arteries, JACC Cardiovasc. Interventions 7 (2014) 768–777.
[9] P.H. Stone, S. Saito, S. Takahashi, Y. Makita, S. Nakamura, T. Kawasaki, A. Takahashi, T. Katsuki, A. Namiki, A. Hirohata, T. Matsumura, S. Yamazaki, H. Yokoi, S. Tanaka, S. Otsuji, F. Yoshimachi, J. Honye, D. Harwood, M. Reitman, A.U. Coskun, M.I. Papafaklis, C.L. Feldman, Prediction of progression of coronary artery disease and clinical outcomes using vascular profiling of endothelial shear stress and arterial plaque characteristics: the PREDICTION Study, Circulation 126 (2012) 172–181.
[10] Y.S. Chatzizisis, A.U. Coskun, M. Jonas, E.R. Edelman, C.L. Feldman, P.H. Stone, Role of endothelial shear stress in the natural history of coronary atherosclerosis and vascular remodeling: molecular, cellular, and vascular behavior, J. Am. Coll. Cardiol. 49 (2007) 2379–2393.
[11] J.J. Wentzel, Y.S. Chatzizisis, F.J. Gijsen, G.D. Giannoglou, C.L. Feldman, P.H. Stone, Endothelial shear stress in the evolution of coronary atherosclerotic plaque and vascular remodelling: current understanding and remaining questions, Cardiovasc. Res. 96 (2012) 234–243.
[12] C.V. Bourantas, M.I. Papafaklis, A. Kotsia, V. Farooq, T. Muramatsu, J. Gomez-Lara, Y.J. Zhang, J. Iqbal, F.G. Kalatzis, K.K. Naka, D.I. Fotiadis, C. Dorange, J. Wang, R. Rapoza, H.M. Garcia-Garcia, Y. Onuma, L.K. Michalis, P.W. Serruys, Effect of the endothelial shear stress patterns on neointimal proliferation following drug-eluting bioresorbable vascular scaffold implantation: an optical coherence tomography study, JACC Cardiovasc. Interventions 7 (2014) 315–324.